論 文

[2145] FAILURE CRITERIA AND NONLINEAR DYNAMIC ANALYSIS OF CONCRETE SLABS UNDER IMPULSIVE LOADS

Michael William KING*, Ayaho MIYAMOTO* and Hiroki MASUI*

1. INTRODUCTION

Understanding the ultimate behaviors of concrete structures under impulsive loads can be considered as a first step forward towards designing impact resistible structures. In this study, an analytical method based on the layered finite element procedure with provision for material nonlinearity, elasto-plasticity, cracking in concrete elements and the loading and unloading phenomena is proposed for studying the ultimate behaviors and failure mechanisms of concrete slabs under impulsive loads. A triaxial failure criterion is also applied in the analysis to consider the various failure modes associated with impulsive loadings. Verification of the analytical procedure is carried out through comparisons with experimental results.

2. FAILURE CRITERION

2.1 FAILURE CRITERION BASED ON OTTOSEN'S MODEL

The failure criterion applied here is the triaxial failure criterion for plain concrete which was proposed by Ottosen [1]. The failure surface for Ottosen's Model (four-parameter model) can be expressed as,

$$f(\rho,\sigma_m,\theta) = \rho - \rho_f(\sigma_m,\theta) = 0 \ , \quad |\theta| \leqq 60^\circ \qquad \cdots\cdots(1)$$

where, $\rho=\sqrt{2J_2}$:stress component perpendicular to the hydrostatic axis. $\cdots\cdots(2)$

$$\rho_f(\sigma_m,\theta)= \frac{1}{2a}[-\sqrt{2}\cdot\lambda+\sqrt{2\cdot\lambda^2-8a(3b\cdot\sigma_m-1)}]: \text{ failure envelope on deviatoric planes.} \qquad \cdots\cdots(3)$$

$\sigma_m = I_1/3$: octahedral mean stress. $\cdots\cdots(4)$

I_1, J_2, θ : stress invariants.

$$\lambda = \begin{cases} k_1\cdot\cos\left[\frac{1}{3}\cos^{-1}(k_2\cdot\cos(3\theta))\right] & ;\text{for } \cos(3\theta)\geqq 0 \\ k_1\cdot\cos\left[\frac{\pi}{3}-\frac{1}{3}\cos^{-1}(-k_2\cdot\cos(3\theta))\right] & ;\text{for } \cos(3\theta)<0 \end{cases} \qquad \cdots\cdots(5)$$

In the above equations, a, b, k_1 and k_2 are constants calibrated from biaxial and triaxial test results reported in the literature. In this study, $\overline{f_t}$ $(= f_t/f_c')$ = 0.12 is selected for the analytical procedure and the corresponding values for the four parameters are a=0.9218, b=2.5969, k_1=9.9110, k_2=0.9647.

* Department of Civil Engineering, Kobe University

where, f_c' : uniaxial compressive strength of concrete
f_t : uniaxial tensile strength of concrete

The Ottosen model is known to have both a parabolic $\tau_{oct} \sim \sigma_{oct}$ relation and also θ-dependance. It is also capable of reproducing all the main features of the triaxial failure surface.

2.2 YIELD CRITERION

The yield criterion for concrete is usually assumed on the basis of the known failure criterion. In earlier plasticity models, the yield surface is assumed to be a proportionally reduced shape of the failure surface as shown in Fig.1(a). It is found that this assumption is inadequate for concrete materials. It is assumed here that no plastic zone exists in the pure tensional region of concrete.

A nonuniform hardening plasticity model proposed by Han and Chen [2] is applied here. A schematic representation of the model employed is shown in Fig.1(b). During hardening, the loading surface expands and changes its shape gradually from the initial yielding surface to the failure surface.

A plastic potential other than the loading function (nonassociated flow rule) is applied here in view of the fact that inelastic volume contraction at the beginning of yielding and volume dilatation at the ultimate stages are known to occur in concrete. The Drucker-Prager type of potential is used here.

2.3 CRITERIA OF LOADING AND UNLOADING

The loading and unloading criteria in stress space can be expressed as,

$$f = 0 \text{ and } \frac{\partial f}{\partial \sigma_{ij}} \cdot d\sigma_{ij} > 0 \rightarrow \text{loading} \quad ; \ d\sigma^p_{ij} \neq 0 \qquad \cdots\cdot(6)$$

$$f = 0 \text{ and } \frac{\partial f}{\partial \sigma_{ij}} \cdot d\sigma_{ij} = 0 \rightarrow \text{neutral loading} \quad ; \ d\sigma^p_{ij} = 0 \qquad \cdots\cdot(7)$$

$$f = 0 \text{ and } \frac{\partial f}{\partial \sigma_{ij}} \cdot d\sigma_{ij} < 0 \rightarrow \text{unloading} \quad ; \ d\sigma^p_{ij} = 0 \qquad \cdots\cdot(8)$$

The stress space is assumed to be based on Drucker's stability postulate. Under loading, the stress condition is such that the stress state moves

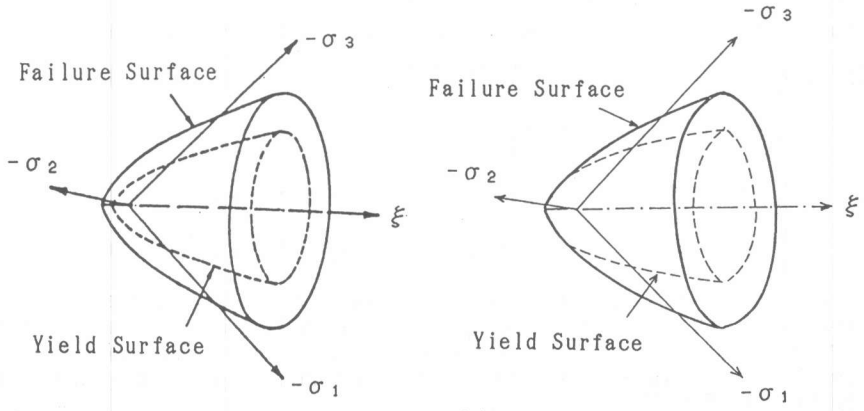

(a) Classical plasticity model (b) Model applied in this analysis

Fig.1 Yield and failure surfaces

outward from one loading surface to another new surface, while under neutral loading the stress point moves along a particular loading surface. The stress state is assumed to move inwards according to the former loading condition to a previous loading surface during unloading. Only the elastic strain components will decrease during unloading.

3. ANALYTICAL PROCEDURE

A 2-dimensional step-by-step finite element method is developed for analysis of reinforced concrete slabs subjected to dynamic impulsive loads. The Newmark-β method is employed to solve the equations of motion during discrete time intervals [3].

3.1 LAYERED FINITE ELEMENT METHOD

Reinforced concrete slabs with doubly reinforced sections are modeled using the layered finite element procedure as shown in Fig.2. The slab is divided into 8 hypothetical layers, 6 of concrete and 2 of reinforcement. The layering approach allows the strains and stresses to be varied with member thickness and permits the inclusion of steel reinforcement at proper levels within the slab.

The finite element employed here is the 4-node rectangular element. Each element nodal-point has 5 degrees of freedom, i.e., inplane displacements (u,v), transverse displacement (w) and sectional rotations around the x and y axes (θ_x,θ_y). The element is considered to consist of the inplane, plate bending and coupling effects. It is considered here that the extensional-bending coupling effect becomes more pronounced due to the shifting of the neutral axis as cracks progress through the concrete slab.

The total strains for each layer is considered to be made up from the inplane element strains $\{\varepsilon_e\}$ and the plate bending related strains $\{\varepsilon\}$. The inplane element strains are constant throughout the thickness of the slab but the strains caused by plate bending varies as the layer separates from the middle surface (reference surface). The total strains for each layer can be expressed as,

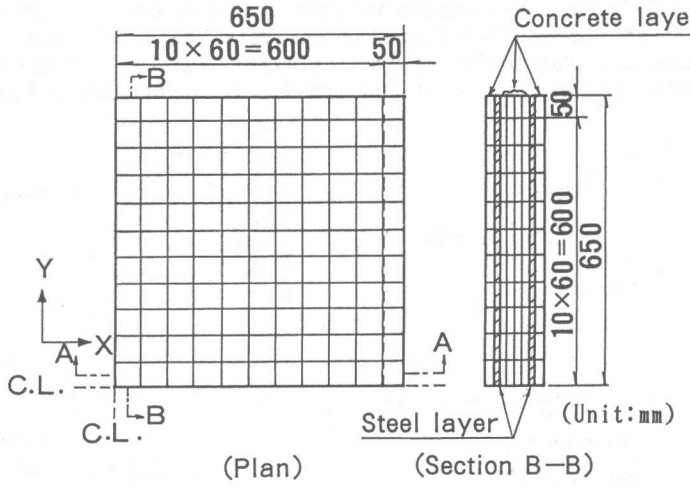

Fig.2 Layered finite element meshes

$$\{\varepsilon_T\} = \{\varepsilon_\theta\} + z\cdot\{\varepsilon\} \qquad \cdots(9)$$

where z is the distance from the reference surface.

The neutral axis is assumed to act at the center of the elastic portion of the slab, expressed by the following equations,

$$e_x = \frac{(1/2)E_c\cdot t^2 + E_s\cdot\Sigma A_{sxi}\cdot Z_{sxi}}{E_c\cdot t + E_s\cdot\Sigma A_{sxi}}\ ,\quad e_y = \frac{(1/2)E_c\cdot t^2 + E_s\cdot\Sigma A_{syi}\cdot Z_{syi}}{E_c\cdot t + E_s\cdot\Sigma A_{syi}} \qquad \cdots(10)$$

where, e_x, e_y : the neutral axes in the x and y directions, respectively.
E_c, E_s : concrete and reinforcement moduli of elasticity, respectively.
A_{sxi}, A_{syi} : average cross-section per unit length in the x, y directions for the i th layer of reinforcement, respectively.
Z_{sxi}, Z_{syi} : distance from the middle of i th layer to the top surface of slab in the x, y directions, respectively.
t : slab thickness.

The total stiffness matrix for the composite element is obtained by integrating the stiffness matrix for each layer and summing up for the total stiffness. The effects of transverse shear stresses in moderately thick plates are considered to affect the ultimate behaviors of concrete slabs such as the crack distribution. The transverse shear stresses for each element are calculated from the equations of equilibrium at each time interval which can be expressed by,

$$\frac{\partial\sigma_x}{\partial x} + \frac{\partial\tau_{xy}}{\partial y} + \frac{\partial\tau_{xz}}{\partial z} = 0\ ,\qquad \frac{\partial\sigma_y}{\partial y} + \frac{\partial\tau_{xy}}{\partial x} + \frac{\partial\tau_{yz}}{\partial z} = 0 \qquad \cdots(11)$$

The transverse shear stresses can be obtained by direct integration of the equations of equilibrium [4],

$$\tau_{xz} = -\int\left(\frac{\partial\sigma_x}{\partial x} + \frac{\partial\tau_{xy}}{\partial y}\right)\cdot dz\ ,\qquad \tau_{yz} = -\int\left(\frac{\partial\sigma_y}{\partial y} + \frac{\partial\tau_{xy}}{\partial x}\right)\cdot dz \qquad \cdots(12)$$

3.2 VERIFICATION OF ANALYTICAL PROCEDURE

Results of experimental tests carried out on reinforced concrete slabs are used to verify the validity of the calculations. Details of the testing procedure can be found in [5]. The types of concrete slabs tested are the *normal strength* reinforced concrete (RC) slabs and *high strength* reinforced concrete (HRC) slabs. The impulsive load function measured during experiments are digitalized and applied into the analysis. Material test results such as Young's modulus, Poisson's ratio, uniaxial material characteristics from uniaxial compressive (concrete) and tensile (reinforcement) tests are used as

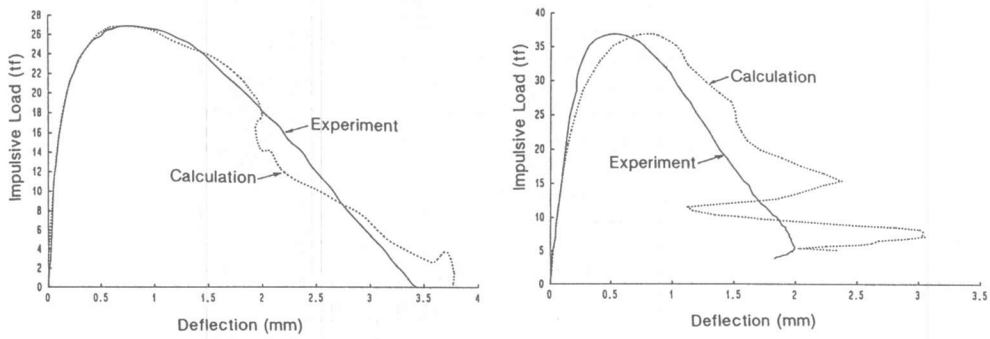

(a) RC slab (b) HRC slab

Fig.3 Impulsive load - midspan deflection function

the input data for the various materials. It should be noted here that the uniaxial material test results are converted into the triaxial effective stress-effective strain relation before application into the calculations [4].

Figs.3(a) and (b) show the impulsive load versus midspan deflection curves for the calculations and experiments of RC and HRC slabs, respectively. Fig.3.(a) shows that the calculations give a very good approximation of the ultimate behaviors of RC slabs especially until the point of maximum impulsive load. The difference between the calculated values and the experiment begin to appear after the maximum impulsive load, i.e., when the unloading process begins. The result for the HRC slab is shown in Fig.3(b). A difference in the curves can be noticed after cracking in the HRC slab. The calculation predicts a larger amount of deflection but on the overall, the response is similar to the experimental result. Some vibrational effects at the final part of the curve are predicted in the calculations due to self-excitation of the slab after unloading. The reason can be attributed to the fact that the Ottosen failure model might not be suitable for high strength concrete.

4. ANALYSIS OF RC SLABS UNDER IMPULSIVE LOADS

The effects of loading rates on RC slabs is studied analytically here. The term *loading rate* is taken as the average gradient of a single-wave impulsive load-time function. The calculations are carried out until failure occurring in the slabs. Failure is defined here as the point at which concrete crushing occurs, or at the point where deflection decreases even with an increase in the impulsive load.

The distribution of deflection for two types of loading rates are shown in Fig.4. The bold lines show the deflection at failure while the broken lines are those at a stage before failure. Fig.4(a) shows the results of a slow loading rate. The failure mode in this case can be considered to be the flexural failure type. Deflection is spread at an equal ratio through the slab in the transverse and longitudinal directions. It can be considered that the total energy from the impulsive load is spread through the entire structure and total structural failure is expected. Fig.4(b) shows the deflection curves in the transverse and longitudinal directions for a high loading rate. The

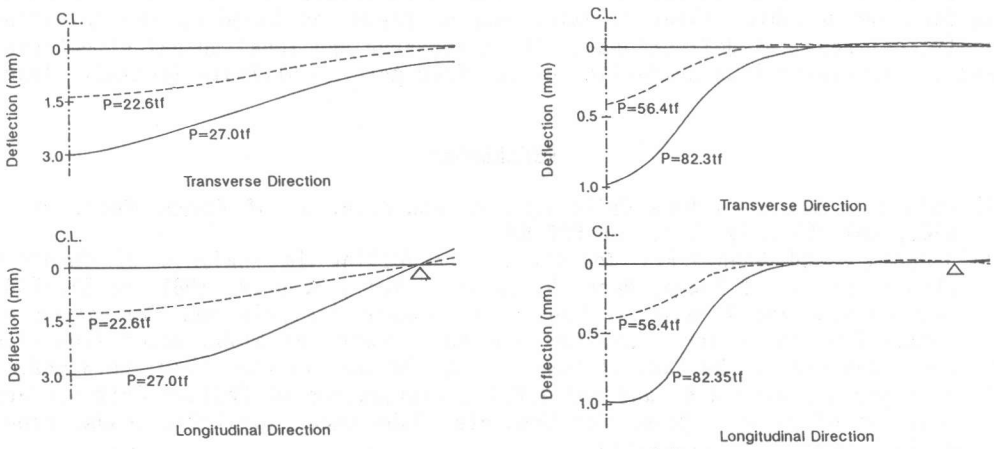

(a) Low loading rate (v_L=7.5tf/msec)

(b) High loading rate (v_L=139.2tf/msec)

Fig.4 Deflection for different loading rates

curves can be classified as those of punching shear failure. Unlike bending failure, local failure at midspan occurs here and it can also be noticed that the amount of deflection is much smaller here. Almost no deflection is noticed at the ends near the supports of the slab.

Fig.5 shows the impulsive load-deflection curves up to failure calculated for various loading rates. The shape of the curves from zero to ultimate impulsive load can be classified into those of bending failure and shear failure. The shear failure type has a larger gradient with small deflection and also a high impulsive load at failure. On the other hand, the curve for flexural failure has a smaller gradient which decreases gradually. The deflection at failure is larger but the failure load is smaller when compared to those of the shear type failure. From all the curves, a failure envelope for concrete slabs under impulsive loads can be assumed as shown by the dotted lines in Fig.5.

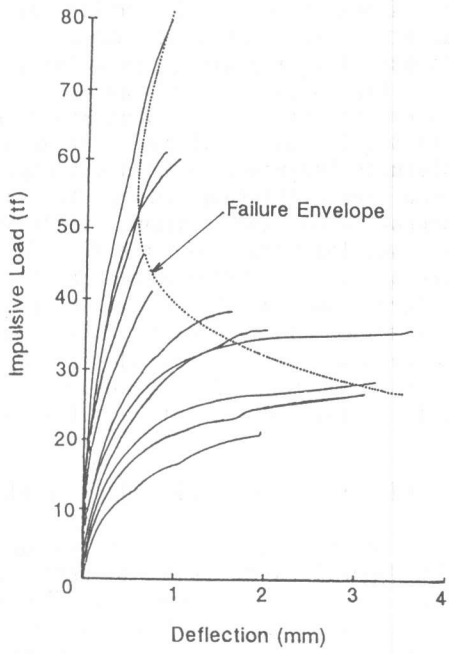

Fig.5 Impulsive load - midspan deflection function (Analysis)

5. CONCLUSIONS

The main conclusions from this study can be summed up as:

(1) The layered finite element method together with the Ottosen failure model and the Drucker-Prager plastic potential is capable of giving very good predictions of the ultimate behaviors for RC slabs under impulsive loads. The failure mechanisms predicted agree very well with the experimental results.

(2) The failure modes for RC slabs under soft impulsive loads, i.e., bending failure and punching shear failure, can be predicted based on the following analytical results: deflections in the transverse and longitudinal directions, and the impulsive load-deflection curves from zero to ultimate impulsive load.

REFERENCES

1) Ottosen,N.S.: A Failure Criterion for Concrete, J. of Engng. Mech. Div., ASCE, Vol.103(EM4), 1977, pp.527-535.
2) Han,D.J. and Chen,W.F.: Constitutive Modelling in Analysis of Concrete Structures, J. of Engng. Mech. Div., ASCE, Vol.113, No.4, 1987, pp.577-593.
3) Miyamoto,A. and King,M.W.: Nonlinear Dynamic Analysis and Evaluation of Impact Resistance for Reinforced Concrete Beams and Slabs under Impulsive Load, Memoirs of the Fac. of Engng., Kobe University, Nov.1989, pp.37-62.
4) Miyamoto,A., King,M.W. and Fujii,M.: Investigation of Failure Criteria and Analysis of Failure Modes for Concrete Slabs under Impulsive Loads, Proc. of JSCE (under contribution)
5) Miyamoto,A., King,M.W. and Masui,H. : Non-Linear Dynamic Analysis and Evaluation of Impact Resistance of Reinforced Concrete Slabs under Impulsive Load, Proc. of the JCI, Vol.11, No.2, 1989, pp.643-648.